

# Collinear superjogs and the low-stress response of fcc crystals

B. Devincere,<sup>a</sup> L. Kubin<sup>a,\*</sup> and T. Hoc<sup>b</sup>

<sup>a</sup>Laboratoire d'Etude des Microstructures, UMR 104, CNRS-ONERA, 29 Av. de la Division Leclerc, 92322 Châtillon Cedex, France

<sup>b</sup>Laboratoire MSSMat, UMR 8570 CNRS, Ecole Centrale Paris, Grande Voie des Vignes, 92295 Châtenay-Malabry Cedex, France

Received 21 June 2007; revised 23 July 2007; accepted 25 July 2007

The mutual interactions of dislocation lines containing collinear superjogs are investigated in face-centered cubic crystals by dislocation dynamics simulations in single slip and for various loading axes. The examination of the dislocation microstructures, dislocation densities and stress–strain curves allows the origin of work hardening during stage I to be clarified and explains the unusual hardening that is observed experimentally in [001] crystals at low stresses.

© 2007 Acta Materialia Inc. Published by Elsevier Ltd. All rights reserved.

**Keywords:** Plastic deformation; Hardening; Dislocation microstructure; Dislocation dynamics; Collinear superjogs

The objective of this work is to examine by three-dimensional (3-D) dislocation dynamics (DD) simulations the low-stress interactions of dislocations, typically in easy glide conditions. A first motivation consists in obtaining microstructural information complementing a model that was proposed for stage I in face-centered cubic (fcc) crystals [1]. This model is based on early studies of stage I hardening (see Ref. [1] for a general discussion), specifically on those which emphasize the stress-driven annihilation of the screw dislocation density. These annihilations leave dislocation segments in the cross-slip plane, which are called here collinear superjogs (the term “collinear” indicates that they have same Burgers vector as the primary dislocations). The very strong interaction between primary and collinear lines [2] is then held responsible for stage I hardening. A second motivation arises from the high strain hardening specific to [001] crystals at low stresses, which is discussed in the concluding part.

During stage I, the activation energy for the mutual annihilation of screw dislocations gliding in neighboring planes is mostly provided by mechanical work. It then requires quite large interaction stresses and short approach distances, typically 6–10 nm in copper [3,4]. Annihilations are nevertheless made possible by the very long mean free path of the dislocations, which is about 1 mm [5]. As DD simulations cannot account for such

mean free paths, the basic idea underlying the present work is to assume that cross-slip events have occurred from the start, producing a small initial density of collinear superjogs, and to simulate the subsequent interactions between superjogs and primary dislocations. For this purpose, DD simulations were carried out on configurations containing an initial density of superjogs and in the absence of cross-slip.

We first describe an important property of collinear superjogs that was observed in DD simulations. In Figure 1, snapshots extracted from a model configuration show the intersection of a collinear edge segment by attractive primary segments. At each interaction, collinear jogs are extracted from the collinear segment and transferred to the mobile lines. This process results in the dissemination of a number of small collinear jogs in the microstructure, which move along the direction of the primary Burgers vector. One can further check from Figure 1 that these intersections do not modify the edge component of the superjog density.

Model DD simulations (see Refs. [1,6]) were devised to investigate microstructural evolutions in the conditions described above. The dimensions of the elementary cell are  $4.3 \times 4.9 \times 5.9 \mu\text{m}^3$  and periodic boundary conditions are used. The initial density consists of two large prismatic loops of opposite sign made up of two primary segments of Burgers vector  $\mathbf{b} = \pm 1/2[101]$  and length  $20 \mu\text{m}$ , connected by two collinear segments of length  $2 \mu\text{m}$ . The corresponding total density is  $7 \times 10^{11} \text{m}^{-2}$ , which is typical of the end of stage I, and it contains 10% of collinear superjogs. A strain rate of  $1 \text{s}^{-1}$  is

\* Corresponding author. Tel.: +33 1 46 73 4449; fax: + 33 1 46 73 4155; e-mail: [ladislas.kubin@onera.fr](mailto:ladislas.kubin@onera.fr)

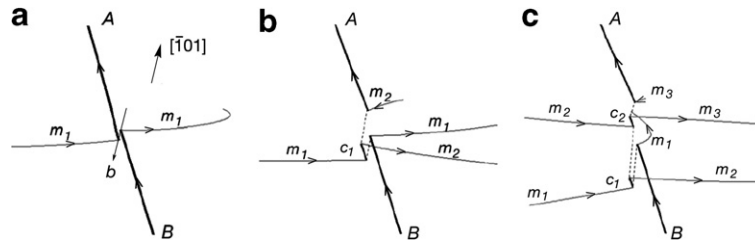


**Figure 1.** The primary slip system is  $[\bar{1}01](111)$  and the cross-slip system is  $[\bar{1}01](1\bar{1}1)$ . The normal to the view plane is a few degrees away from  $[\bar{1}01]$ . Three attractive primary mobile segments ( $m_i$ ) successively cut a collinear segment  $AB$ . All segments have the same Burgers vector,  $1/2[10\bar{1}]$ , and their line directions are indicated. (a) Upon interaction between  $AB$  and  $m_1$ , annihilation occurs along the direction of  $b$ . After reaction, the two lines have exchanged segments. (b) A second intersection occurs with primary line  $m_2$ , which takes away a collinear jog ( $c_1$ ) that moves along the direction of  $b$ . (c) A third incoming segment incorporates another collinear jog ( $c_2$ ).

applied along two single slip orientations,  $[\bar{1}23]$  and  $[\bar{1}28]$ , and two high symmetry orientations,  $[001]$  and  $[\bar{1}11]$ . The model material is copper.

For the  $[\bar{1}23]$ ,  $[\bar{1}28]$  and  $[\bar{1}11]$  orientations, the simulated microstructures consist of dipolar or multipolar bundles elongated along the primary edge direction, connected by a few long segments that trail prismatic dipolar loops (Fig. 2). These arrangements are formed by the intersection of collinear superjogs with mobile primary lines and further with various by-products formed by these interactions. After a resolved plastic strain  $\gamma_p = 0.8\%^1$ , the bundles have lengths of several microns in the primary slip plane, while the length of the isolated prismatic loops is slightly less than  $1\ \mu\text{m}$ . In accordance with a mechanism conjectured in Ref. [7], the dimensions of the prismatic loops are continuously refined during the simulations. The simulated patterns are very similar to those formed during stage I (see e.g., Ref. [8] and the review articles [5,9]) and during the early stages of cyclic deformation [10]. Thus, the present simulations provide an efficient bypass for producing realistic stage I microstructures.

The  $[001]$  orientation is characterized by a particular behavior. The simulated microstructures are globally similar to the ones described above, except that the prismatic loops exhibit squarish shapes and the dislocation bundles are no longer elongated but rather isotropic. In addition, some collinear segments appear to be dragged by the moving primary dislocations, up to the point that they can reach the critical condition for operating as dislocation sources. This is illustrated by Figure 3. The collinear segment  $BC$  is connected at one extremity  $C$  to a short immobile segment, whereas its other extremity is connected to a mobile segment  $AB$  (Fig. 3a). The latter drags the collinear segment and elongates it. For this orientation, the Schmid factors are the same in the slip and cross-slip planes. As a consequence, when the two segments reach equal lengths (Fig. 3b), their connecting node behaves as a pinning point. The collinear segment can then expand in an irreversible manner provided it reaches its critical stress before the mobile one. Configurations are also met in which the mobile segment and the collinear jog move in a cooperative manner, which involves a smaller drag-

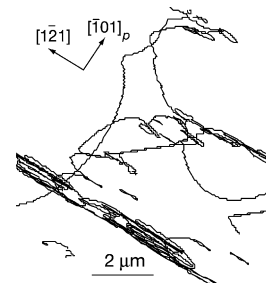


**Figure 2.** Thin film of thickness  $3\ \mu\text{m}$  extracted from a simulated microstructure after a plastic strain of  $0.8\%$  along a  $[\bar{1}23]$  stress axis. The viewpoint is slightly tilted from the primary slip plane around the primary edge direction,  $[1\bar{2}1]$ . The projected direction of the primary screw is also indicated.

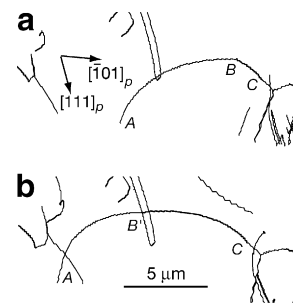


**Figure 3.** Thin film of thickness  $3\ \mu\text{m}$  extracted from a simulated microstructure obtained under a  $[001]$  loading axis. The projected directions of the primary Burgers vector and of the normal to the primary slip plane are indicated. (a) The collinear jog  $BC$  is dragged by a primary segment  $AB$ . (b) The node  $B$  moves to  $B'$ , along the  $[10\bar{1}]$  direction, and the collinear jog is extended. In the next simulation step, it expands in an irreversible manner.

ging effect and suppresses multiplication in the cross-slip plane.

The outputs of the simulations confirm that all orientations behave in the same manner except  $[001]$ . Figure 4a and b shows, respectively, the strain dependence of the dislocation densities in the primary and collinear slip systems and the stress vs. plastic strain behavior for the  $[001]$  and  $[\bar{1}23]$  orientations. The large fluctuations that can be seen on these curves arise from local slip bursts. They are intrinsic to plastic flow and their amplitude decreases with increasing simulated volume.

<sup>1</sup> Artifacts arising from periodic boundary conditions start appearing at this strain value.

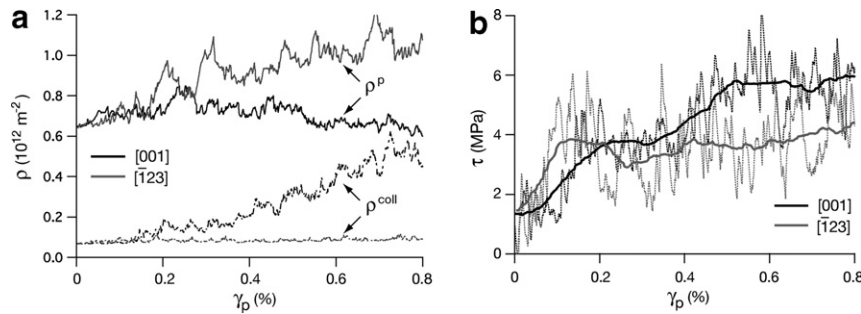


**Figure 4.** (a) Evolution of primary and collinear dislocation densities as a function of plastic strain. The collinear density is constant for the  $[\bar{1}23]$  orientation, whereas it continuously increases for the  $[001]$  orientation. The total density is the same for both orientations. (b) Simulated stress vs. plastic strain curves for the  $[\bar{1}23]$  and  $[001]$  orientations, showing the occurrence of an additional hardening in the last case. As there are strong stress fluctuations, a sliding average method is used to draw smoother curves.

We discuss first easy glide conditions, taking  $[\bar{1}23]$  as reference. As expected from the considerations developed above, the collinear density remains constant during the whole simulated test (Fig. 4a). In parallel, the flow stress increases. In simple terms, hardening is found to arise from a combination of (i) forest hardening of the primary density by the collinear superjogs; (ii) the interaction of jogged primary dislocations lines with an increasing number of prismatic loops, either isolated or stored in the multipolar bundles; and (iii) jog dragging plus various dipolar interactions. This complex behavior suggests checking the hypothesis made in Ref. [1] that all these contributions to Taylor hardening can be lumped into a single average self-interaction coefficient,  $a'_0$ . One can draw from Figures 4a and b an upper value for this dimensionless coefficient from the Taylor-like form  $\tau = \mu b \sqrt{a'_0 \rho}$  assuming that the total density,  $\rho$ , is almost entirely made up of stored dislocations. In the last 0.2% plastic strain range of the simulation, where the collinear density is about 6% of the total density, a statistical analysis of the raw data yields  $a'_0 = 0.124 \pm 0.04$  for copper ( $\mu = 42$  GPa,  $b = 0.256$  nm). Although the value of this coefficient depends on the initial values of the collinear jog density, the present value was chosen in order to match a theoretical prediction [1]. Considering the critical stresses for primary and  $[01\bar{1}]$  ( $\bar{1}\bar{1}1$ ) conjugate slip in conditions of symmetrical duplex slip, it was shown that one should have  $a'_0 \approx a_2$  in copper, where  $a_2$  is the interaction coefficient associated with conjugate duplex slip. From Ref. [6], one has  $a_2 = 0.122 \pm 0.012 \approx a'_0$  for a total density of about  $10^{12} \text{ m}^{-2}$ , like the ones considered here. More generally, as collinear superjogs are created by cross-slip events, the value of  $a'_0$  may depend on the stacking fault energy.

The relevance of the present results with respect to stage I in fcc crystals deserves discussion. Stage I strain hardening is approximately linear, which confirms that the self-hardening coefficient can, by approximation, be taken as a constant. It has been further experimentally observed that during stage I of copper, one finds in the dislocation bundles a small density of secondary dislocations, which is a constant fraction of the primary density [11]. This fraction is not precisely known and its experimental estimates range from a few percent to 10% according to Steeds [8] and other authors (see the review by Basinski and Basinski [5]). Furthermore, Essmann [12] has shown that the secondary density mostly con-

tains collinear superjogs, which is in qualitative agreement with the results drawn from the present simulations. To summarize, the present model simulation allows typical stage I dislocation microstructures to be determined and the previous hypotheses regarding the self-interaction coefficient to be checked.

We now return to the  $[001]$  orientation. One can see from Figure 4a that the collinear density continuously increases with plastic strain as a consequence of multiplication events (Fig. 3). In parallel, the primary density decreases due to rearrangements induced by collinear interactions. Eventually, the two densities are reaching almost the same value, which means that conditions of duplex collinear slip are nearly achieved. The flow stress increases significantly more than for the other orientations (Fig. 4b), up to about  $\tau \approx 5.5 \text{ MPa}^2$  at the end of the simulation. This results from the large value of the interaction coefficient ( $a_{\text{coli}} = 0.63$ ; cf. Ref. [6]) associated with collinear interactions, as compared with the value determined above for  $a'_0$ .

From the discussion of Figure 3, it appears that collinear jogs can multiply provided that they are dragged by primary edges. In addition, the Peach–Koehler forces on the two segments must be equal and opposite, a condition that is only realized for loading along the  $[001]$  and  $[\bar{1}11]$  orientations. The reason why duplex collinear slip is only observed for the  $[001]$  orientation is essentially crystallographic. A cross-slipping screw dislocation can adopt two possible directions of motion of opposite sign in its cross-slip plane. This results in the formation of two possible types of superjogs (Fig. 5), which are traditionally called acute and obtuse [13]. Under the high interaction stresses that induce mechanical cross-slip in stage I, these two configurations are produced in statistically equal amounts. This symmetry is also respected in the initial conditions of the DD simulations because each superjog of a prismatic loop is acute with respect to one of its neighbors and obtuse with respect to the other.

In a first step, we now examine the directions of motion of superjogs under a stress applied along the  $[001]$  direction. They are shown in Figure 5, as derived from

<sup>2</sup>A constant friction stress of 0.5 MPa, which was introduced for technical convenience, was subtracted.

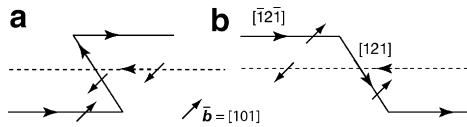


**Figure 5.** Acute (a) and obtuse superjog (b) on a primary edge dislocation line of Burgers vector  $\mathbf{b}$ . The line directions are indicated. The small arrows indicate the directions of motion of the segments under a stress applied along  $[001]$ . The dotted line is a primary edge that interacts with the collinear superjogs.

the Peach–Koehler relation. The acute jog is resistive, and it was checked on simulated configurations that source configurations like the one shown in Figure 3, involve acute jogs. The obtuse jog (Fig. 5b), which is of the opposite sign, moves in a cooperative manner with the primary edge segments. Redoing the same analysis for a stress applied along  $[\bar{1}11]$ , one finds that the primary edges are still moving in the same direction, whereas the direction of motion of the collinear segments is reversed. The reason is that the normal to the cross-slip plane,  $[\bar{1}11]$ , makes an angle smaller than  $\pi/2$  with  $[001]$  and larger than  $\pi/2$  with  $[\bar{1}11]$ . As a consequence, the Schmid factor and the Peach–Koehler forces in the cross-slip plane change sign (this geometrical effect was recently discussed within a different context [13]). Therefore, at this step, collinear multiplication can occur on acute, resistive superjogs for the  $[001]$  orientation, as is observed, and on obtuse, resistive superjogs for the  $[\bar{1}11]$  orientation.

We can now examine the interaction of the two types of superjogs with an incoming dislocation that moves in the direction opposite to that of the primary edges (dashed line in Fig. 5a and b). Simple calculations, as well as simulations, for various orientations of the lines show that obtuse superjogs interact in an attractive manner with incoming primary dislocations and are the most reactive. Then, from an initial microstructure that includes superjogs of both types in equal density, plastic deformation preferentially produces reactions with the obtuse superjogs irrespective of the loading direction. By considering the successive reactions of each type of superjog with mobile dislocations, one can easily verify that they generate acute and obtuse superjogs in equal numbers. Hence, at each generation of reactions, obtuse superjogs are decomposed into acute jogs that tend to remain in the microstructure and obtuse superjogs that are again decomposed. As a consequence, obtuse superjogs should progressively disappear from the microstructure. Statistics of jog types performed at the end of DD simulations confirm this prediction. Acute, resistive jogs are 2.8 times more frequent than obtuse jogs for the  $[001]$  orientation, and acute, cooperative jogs are 3.2 times more frequent for the  $[\bar{1}11]$  orientation. As a consequence, multiplication via resistive collinear superjogs is likely to be restricted to acute jogs in the  $[001]$  orientation.

The high strain hardening rate of  $[001]$  crystals at low stresses (about  $10^{-2}\mu$ ) is traditionally discussed in terms of long- or short-range interactions between dislocations [9,14,15]. There are, however, conflicting reports about

the number (four or eight), nature and spatial distribution of the active slip systems [16,17]. Detailed slip trace analyses, notably those by Vorbrugg et al. [18], addressed this problem. Although eight slip systems are active on average, all volume elements do not deform in the same manner. Locally, one finds most often two sets of slip planes and two slip systems in the cross-slip position. Then, the activation of cross-slip (collinear) systems, the high interaction strength of which was recently demonstrated [2,6], suggests the occurrence of an additional contribution to strain hardening. It may also explain the observation of an abrupt drop in the strain hardening rate with misorientations as small as a few degrees [15]. The present results clearly need to be confirmed by more realistic large-scale DD simulations performed in multislip conditions. Work in this direction is in progress.

The present DD simulations, in which cross-slip is decoupled from further microstructural evolution, bring to light two important low-stress properties of collinear superjogs that are common to all fcc crystals.

1. The interactions between primary lines and a small density of collinear superjogs are responsible for the formation of a dislocation microstructure that is typical of stage I. A global self-interaction coefficient is defined for primary slip, which gives substance to a previously proposed model for stage I hardening.
2. The unusually high work hardening rate observed at low stresses on  $[001]$  fcc crystals is explained by the occurrence of a specific multiplication mechanism which enforces the activation of collinear duplex slip.

- [1] T. Hoc, B. Devincere, L.P. Kubin, in: C. Gundlach et al. (Eds.), *Evolution of Deformation Microstructures in 3-D*, Risoe National Laboratory, Roskilde, 2004, pp. 43–59.
- [2] R. Madec, B. Devincere, L. Kubin, T. Hoc, D. Rodney, *Science* 301 (2003) 1879.
- [3] L.M. Brown, *Philos. Mag. A* 82 (2002) 1691.
- [4] T. Vegge, K.W. Jakobsen, *J. Phys.: Condens. Matter* 14 (2002) 2929.
- [5] S.J. Basinski, Z.S. Basinski, in: F.R.N. Nabarro (Ed.), *Dislocations in Solids*, vol. 4, North-Holland, Amsterdam, 1979, p. 261.
- [6] B. Devincere, L. Kubin, T. Hoc, *Scripta Mater.* 54 (2006) 741.
- [7] P. Veyssi re, *Philos. Mag. Lett.* 81 (2001) 733.
- [8] J.W. Steeds, *Proc. Roy. Soc. A* 292 (1966) 343.
- [9] H. Mughrabi, in: A.S. Argon (Ed.), *Constitutive equations in Plasticity*, MIT Press, Cambridge, MA, 1975, p. 199.
- [10] C. Laird, in: F.R.N. Nabarro (Ed.), *Dislocations in Solids*, vol. 6, North-Holland, Amsterdam, 1983, p. 55.
- [11] J. Gil Sevillano, in: H. Mughrabi (Ed.), *Plastic Deformation and Fracture of Materials*, VCH, Weinheim, 1993, p. 19.
- [12] U. Essmann, *Acta Metall.* 12 (1964) 1468.
- [13] L.P. Kubin, B. Devincere, T. Hoc, *Philos. Mag.* 86 (2006) 4023.
- [14] C. Schwink, E. G ttler, *Acta Metall.* 24 (1976) 173.
- [15] T. Takeuchi, *J. Phys. Soc. Jpn.* 40 (1976) 741.
- [16] R.W.K. Honeycombe, *The Plastic Deformation of Metals*, Edward Arnold, London, 1968, p. 82.
- [17] L.M. Clarebrough, M.E. Hargreaves, *Prog. Metall. Phys.* 8 (1959) 1.
- [18] W. Vorbrugg, H.C. Goetting, C. Schwink, *Phys. Stat. Sol.* (b) 46 (1971) 257.